Thermochromic Magnetic Ionic Liquids from Cationic Nickel(II) Complexes Exhibiting Intramolecular Coordination Equilibrium

Lan, Xue ; Mochida, Tomoyuki ; Funasako, Yusuke ; Takahashi, Kazuyuki ; Sakurai, Takahiro ; Ohta, Hitoshi

(Citation)
Chemistry-A European Journal,23(4):823-831

(Issue Date)
2017-01

(Resource Type)
journal article

(Version)
Accepted Manuscript

Thermochromic Magnetic Ionic Liquids from Cationic Nickel(II) Complexes Exhibiting Intramolecular Coordination Equilibrium

Xue Lan,[a] Tomoyuki Mochida,*[a] Yusuke Funasako,[b] Kazuyuki Takahashi,[a] Takahiro Sakurai,[c] and Hitoshi Ohta[d,e]

Abstract: There are various thermochromic materials, though liquid thermochromic materials are less common. To produce functional thermochromic liquids, we have designed ionic liquids based on cationic nickel complexes with ether side chains, [Ni(acac)($Me_2NC_2H_4NR^1R^2$)]Tf_2N ([**1**]Tf_2N: R^1 = C_3H_6OEt, R^2 = Me, [**2**]Tf_2N: R^1 = C_3H_6OMe, R^2 = Me, [**3**]Tf_2N: R^1 = R^2 = C_3H_6OMe), where acac = acetylacetonate and Tf_2N = $(F_3CSO_2)_2N^-$. The side chains (R^1, R^2) can moderately coordinate to the metal center, enabling temperature-dependent coordination equilibrium in the liquid state. [**1**]Tf_2N is a liquid at room temperature. [**2**]Tf_2N is obtained as a solid (T_m = 352.7 K) but remains liquid at room temperature after melting. [**3**]Tf_2N is a solid with a high melting point (T_m = 422.3 K). These salts display thermochromism in the liquid state, colored red at high temperatures and orange, light blue, or bluish green at lower temperatures, exhibiting concomitant changes in the magnetic properties. This phenomenon is based on temperature-dependent equilibrium between a square-planar diamagnetic species and a paramagnetic species with intramolecular ether coordination.

Introduction

A range of thermochromic materials have been developed to date, which are mostly solids, liquid crystals, polymers, gels or other hybrid materials.[1] They exhibit color changes depending on temperature, and many applications have been realized so far. Thermochromism of organic compounds, metal complexes, and metal salts in solution is also known,[1,2] but liquid thermochromic materials are less common.

The science and technology of ionic liquids (ILs) have attracted much attention over the past few decades.[3] Various functional ILs have been developed, including ILs that change color in response to external stimuli, such as photochromic,[4] electrochromic,[5] solvatochromic,[6] vapochromic,[7] and thermochromic[8] ILs. In particular, thermochromic ILs may be advantageous for applications over conventional thermochromic liquids owing to the characteristics such as non-volatility and ionic conductivity; however, there are only a few examples of pure thermochromic ILs, such as those containing uranyl isothiocyanate anions[8a] or cationic spin-crossover complexes[8b]. Most IL-related thermochromic materials are mixtures,[9] and the mechanism of their thermochromism mostly lies in their temperature-dependent coordination structures. Furthermore, development of magnetic ionic liquids has also attracted attention recently.[10] Considering this background, designing thermochromic magnetic ILs is an interesting target for functionalizing ILs.

In this study, to develop thermochromic ILs that exhibit a concomitant change in magnetic properties, we designed a cationic nickel complex bearing an ether side chain as shown in Figure 1, the formula of which is represented as [Ni(acac)(R-diamine)]$^+$ (acac = acetylacetonate, R = ether side chain). The mixed-ligand complexes [M(acac)(diamine)]$^+$ (M = Cu^{II}, Ni^{II}) are well-known solvatochromic cations with square-planar coordination geometry, which exhibit color changes in solution owing to solvent molecule coordination.[11] In particular, the Ni-containing cation exhibits thermochromism in alcohols based on the equilibrium between the red diamagnetic square-planar species and a blue solvent-coordinated paramagnetic species.[12,13] In the complex shown in Figure 1, the ether side chain incorporated into the solvatochromic complex enables coordination equilibrium without solvent molecules. The closed form is expected to be entropically more stable than the open form at low temperatures, and hence a temperature-dependent shift in the equilibrium is expected. As a basis for this molecular design, we previously synthesized ILs with solvatochromic cations, [M(acac)(R-diamine)]Tf_2N (M = Cu^{II}, Ni^{II}; R = alkyl substituent; Tf_2N = $(F_3CSO_2)_2N^-$), which exhibit vapochromic properties.[7] Furthermore, we synthesized relevant copper-containing ILs with ether side chains and demonstrated that control of their solvatochromism is possible due to side chain coordination.[6] In this study, however, we used nickel as the metal center to incorporate the spin equilibrium mechanism. This is crucial because the corresponding copper complex is paramagnetic regardless of the coordination structure, giving no such spin equilibrium or thermochromism.

[a] X. Lan, Prof. Dr. T. Mochida, Prof. Dr. K. Takahashi
Department of Chemistry, Graduate School of Science
Kobe University
Rokkodai, Nada, Kobe, Hyogo 657-8501 (Japan)
E-mail: tmochida@platinum.kobe-u.ac.jp
[b] Dr. Y. Funasako
Department of Applied Chemistry, Faculty of Engineering
Tokyo University of Science, Yamaguchi
Sanyo-Onoda, Yamaguchi 756-0884 (Japan)
[c] Dr. T. Sakurai
Center for Supports to Research and Education Activities
Kobe University
Kobe, Hyogo 657-8501 (Japan)
[d] Prof. Dr. H. Ohta
Department of Physics, Graduate School of Science
Kobe University
Kobe, Hyogo 657-8501 (Japan)
[e] Prof. Dr. H. Ohta
Molecular Photoscience Research Center
Kobe University
Kobe, Hyogo 657-8501 (Japan)

Supporting information for this article is given via a link at the end of the document.

Herein, we report the synthesis and the thermochromic and magnetic properties of [Ni(L^1)(acac)]Tf_2N ([**1**]Tf_2N), [Ni(L^2)(acac)]Tf_2N ([**2**]Tf_2N), and [Ni(L^3)(acac)]Tf_2N ([**3**]Tf_2N) (L^1 = *N*′-(3′-ethoxy)propyl-*N*,*N*,*N*′-trimethylethylenediamine, L^2 = *N*′-(3′-methoxy)propyl-*N*,*N*,*N*′-trimethylethylenediamine, L^3 = *N*′,*N*′-(3′,3′′-methoxy)dipropyl-*N*,*N*-dimethylethylenediamine), as shown in Figure 2. In these cations, the stability of the closed form, relative to the open form, is expected to increase in the order of [**1**]$^+$ < [**2**]$^+$ < [**3**]$^+$; cation [**2**]$^+$ has smaller steric hindrance than [**1**]$^+$ owing to the shorter alkoxy substituent, facilitating ether coordination. Cation [**3**]$^+$ can more easily accomplish ether coordination because of two side chains, forming five- and six-coordinate structures. The equilibrium between the closed and open forms in these liquids could be monitored through magnetic susceptibility measurements. The liquids also exhibited a color change owing to water absorption, and the structures of the water-coordinated cations were elucidated.

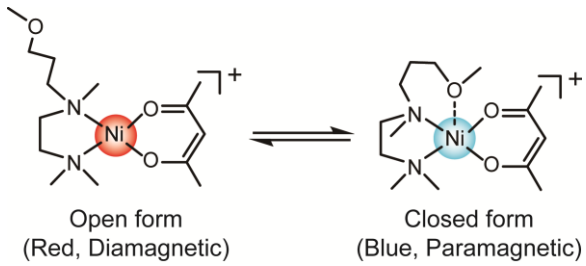

Figure 1. Coordination equilibrium of a cationic mixed-ligand nickel complex with an ether side chain designed in this study.

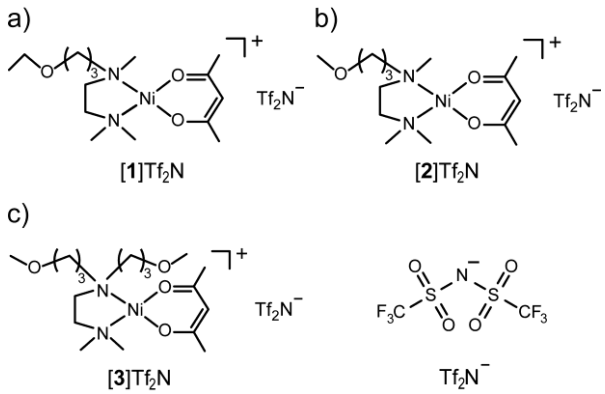

Figure 2. Thermochromic complexes synthesized in this study. (a) [**1**]Tf_2N, (b) [**2**]Tf_2N, and (c) [**3**]Tf_2N. The structure of the Tf_2N anion is also shown.

Results and Discussion

Preparation and properties

[**1**]Tf_2N–[**3**]Tf_2N were synthesized by the reaction of nickel nitrate with diamine and diketonate ligands in alcohol, followed by anion exchange. Their appearance and thermal characteristics are summarized in Figure 3. [**1**]Tf_2N is a red liquid at room temperature. [**2**]Tf_2N is obtained as a light-blue solid, but after melting at T_m = 353 K, it remains a red liquid at room temperature. [**3**]Tf_2N is a bluish-green solid with a high melting point (T_m = 422 K). The melting point increases with increasing relative stability of the closed form in the order of [**1**]$^+$ < [**2**]$^+$ < [**3**]$^+$. The bluish color of the solids indicates that the cations adopt the closed form in the solid state. These salts exhibit thermochromism in the liquid state, as shown in Figure 3, which will be discussed in detail in the following sections.

The liquids of [**1**]Tf_2N and [**2**]Tf_2N exhibit a color change in response to water molecules. They absorbed water molecules when placed in air, changing color from red to light blue in 10 s and in a few minutes, respectively. The faster absorption in the former liquid is probably due to the larger ratio of the open form, as shown later. After water absorption, [**1**]Tf_2N remained a liquid, whereas [**2**]Tf_2N solidified in a few hours, the melting point of which was around 350 K. Of note, the water affinity is the effect of the ether substituent, because the corresponding IL with an alkyl substituent exhibits no such response to water.[7] The absorbed water molecules are fully removed by heating at 70 °C under vacuum for a few hours. The solids of [**2**]Tf_2N and [**3**]Tf_2N did not absorb water. The crystal structures of the water-coordinated species are discussed in the last section.

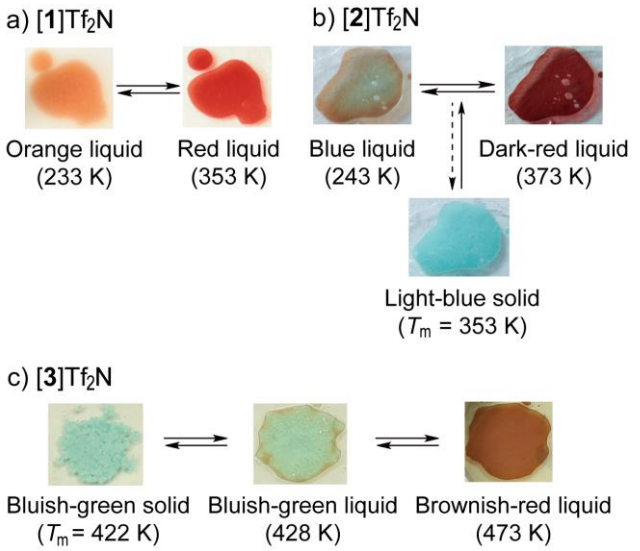

Figure 3. Summary of the thermal characteristics of (a) [**1**]Tf_2N, (b) [**2**]Tf_2N, and (c) [**3**]Tf_2N.

Thermal properties

The thermal properties of [**1**]Tf_2N–[**3**]Tf_2N were investigated by means of differential scanning calorimetry (DSC). The DSC data are listed in Table 1. The DSC traces of [**2**]Tf_2N and [**3**]Tf_2N are shown in Figure 4.

The liquid salt [**1**]Tf_2N does not crystallize, even at low temperatures, undergoing only a glass transition at 229 K. The solid of [**2**]Tf_2N exhibits a phase transition at 160.4 K (ΔS = 1.6 J K^{-1} mol^{-1}) and then melts at 352.7 K (ΔS_m = 98.3 J K^{-1} mol^{-1}) (Figure 4a). The large entropies of fusion for [**2**]Tf_2N are in accordance with the structural change from the closed form to the equilibrium mixture. After melting, the liquid undergoes a

glass transition at 249 K upon cooling. The glass transition temperature is higher than that of [**1**]Tf_2N by 20 K. The value of T_g/T_m is 0.71, in good agreement with the empirical rule (T_g/T_m = 2/3). The liquid undergoes crystallization during the heating process around 280 K. The melting point of [**2**]Tf_2N is higher by 35 K than that of the corresponding Cu complex (T_m = 317.3 K, ΔS_m = 85.5 J K^{-1} mol^{-1}).[6]

The solid of [**3**]Tf_2N undergoes a solid phase transition at 310.0 K (ΔS = 52.8 J K^{-1} mol^{-1}) and then melts at 422.3 K (ΔS_m = 20.3 J K^{-1} mol^{-1}) (Figure 4b). The small melting entropy indicates that the high-temperature phase is an orientationally disordered phase;[14] however, unlike ordinary plastic crystals, anisotropy was observed through a polarized microscope, indicating lower symmetry of the crystal lattice than cubic or hexagonal. The small melting entropy indicates that a dominant portion of the cation maintains chelate coordination just above the melting point. This is also supported by the Vis-NIR spectrum, as shown later.

Table 1. Phase transition temperatures and thermodynamic quantities of [**1**]Tf_2N–[**3**]Tf_2N.

	T_g (K)	T_m (K)	ΔS_m (J K^{-1} mol^{-1})
[**1**]Tf_2N	229		
[**2**]Tf_2N	249	352.7	98.3
[**3**]Tf_2N	–	422.3	20.3

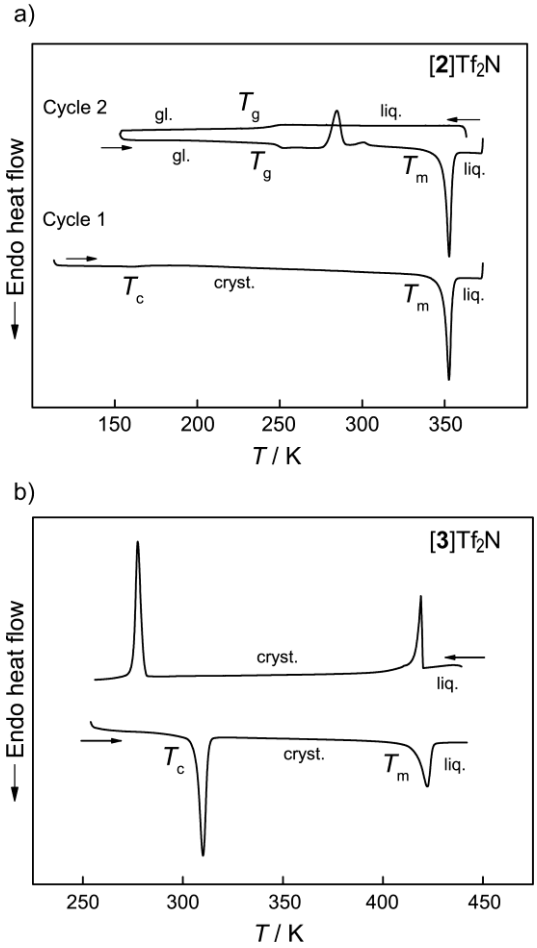

Figure 4. DSC traces of (a) [**2**]Tf_2N and (b) [**3**]Tf_2N.

Thermochromism

[**1**]Tf_2N–[**3**]Tf_2N exhibit thermochromism in the liquid state, based on the equilibrium between the closed and open forms (Figure 1). We also measured the temperature dependence of the Vis-NIR absorption spectra to investigate the equilibrium.

The color of liquid [**1**]Tf_2N gradually changed from red to orange with decreasing temperature from 353 to 233 K (Figure 5a). The color change was fully reversible in this temperature range. No color change was observed below the glass transition temperature (T_g = 229 K), consistent with the freezing of coordination equilibrium. The temperature dependence of its Vis-NIR spectra is shown in Figure 6a. In the spectra of the mixed-ligand solvatochromic Ni^{II} complexes, the d–d transition peak for the red square-planar species appears around 490 nm, and those for the blue solvent-coordinated species appear around 610 and 1040 nm as weak broad peaks with small molar absorbance coefficients.[13] In the spectra of [**1**]Tf_2N, the absorption peak around 490 nm decreases and the absorption around 610 and 1040 nm slightly increases with decreasing temperature. This change corresponds to a decrease in the amount of the open form and an increase in the amount of the closed form at lower temperatures, consistent with the observed color change. The ratios of the two forms are discussed qualitatively in the next section, based on magnetic data. Although the coordination ability of the Tf_2N anion is very weak (*DN* = 5.4),[15] it might be possible that the closed form is weakly coordinated with the anion to form an octahedral coordination geometry; however, the five- and six-coordinate mixed-ligand Ni^{II} complexes cannot be clearly distinguished from the Vis-NIR spectra, as discussed later, and hence we refrain from discussion on this point.

The light-blue solid of [**2**]Tf_2N melted at 353 K to turn into a red liquid. The liquid changed its color from red to blue with decreasing temperature from 373 to 243 K (Figure 5b), exhibiting a more prominent color change than [**1**]Tf_2N. No color change was observed below the glass transition temperature. This liquid undergoes crystallization in the heating process around 280 K, and the resulting solid does not exhibit thermochromism. Therefore, the color change is reversible except in the temperature range where crystallization occurs. The Vis-NIR spectrum of [**2**]Tf_2N is shown in Figure 6b. The temperature dependence in the liquid state is similar to that in [**1**]Tf_2N, but with a much higher ratio of the closed form at each temperature, accounting for the more prominent color change relative to [**1**]Tf_2N. On the other hand, the spectrum of solid

[**2**]Tf_2N exhibits d–d transition peaks at λ_{max} = 607 and 1018 nm (Figure S1a, Supporting Information), which demonstrates that the salt adopts the closed form structure in the solid state.

The bluish-green solid of [**3**]Tf_2N melted at 428 K to become a bluish-green liquid. The liquid gradually turns to brownish-red with increasing temperature, at least up to 473 K, in a reversible manner. The color change occurs in a much narrower temperature range than those in [**1**]Tf_2N and [**2**]Tf_2N. The temperature dependence of the Vis-NIR absorption spectra in the liquid state is consistent with this tendency (Figure 6c). The spectra indicate that the ratio of the closed form (λ_{max} ~ 1000 nm) is still large just after melting, consistent with a small melting entropy and a less prominent color change upon melting. Comparison of [**1**]Tf_2N–[**3**]Tf_2N indicates that the temperature dependence of the ratios of the two species becomes larger in the order of [**1**]Tf_2N < [**2**]Tf_2N < [**3**]Tf_2N. This tendency is consistent with the order of the stability of the closed form relative to the open form, as mentioned in the introduction section, and also the entropy contribution of the two side chains in the case of [**3**]Tf_2N.

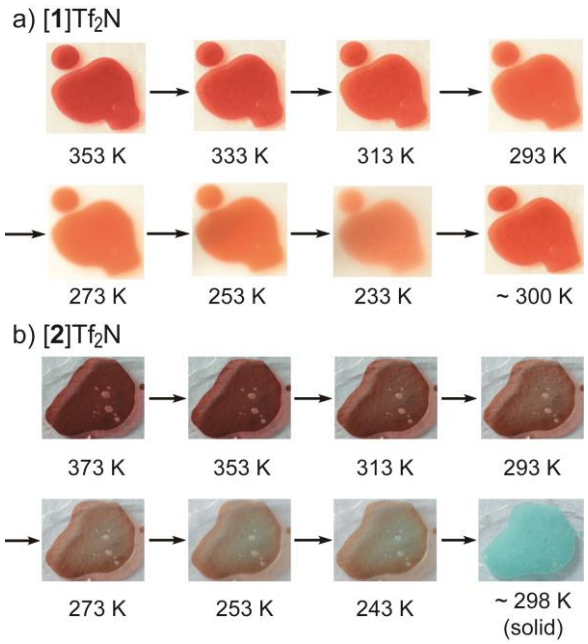

Figure 5. Photographs of (a) [**1**]Tf_2N and (b) [**2**]Tf_2N at different temperatures. The photographs were taken during the cooling process, as indicated by arrows, except for the last ones.

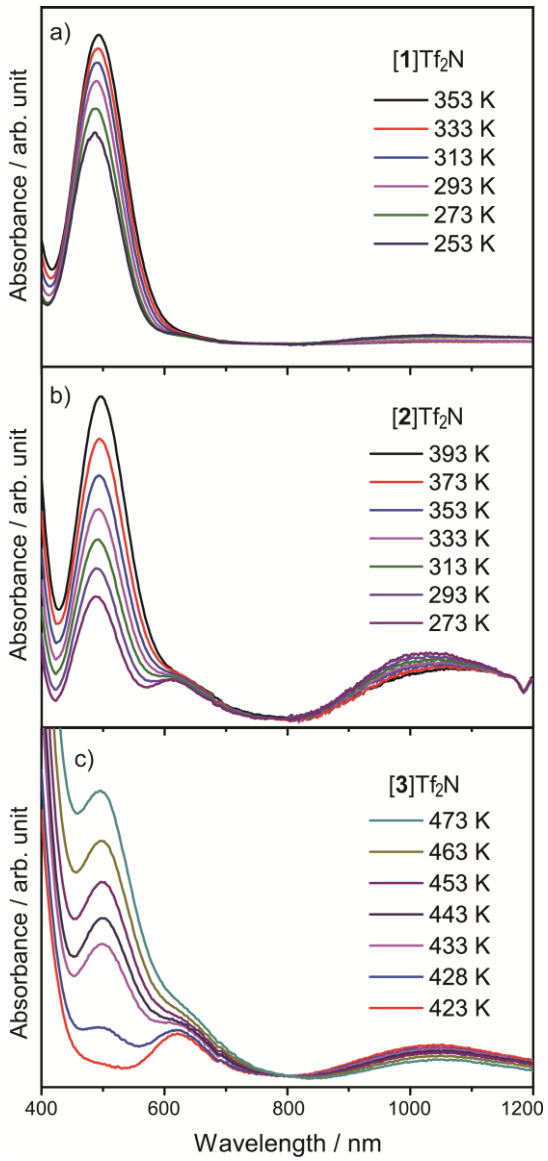

Figure 6. Temperature dependence of the Vis-NIR absorption spectra of (a) [**1**]Tf_2N (353–253 K), (b) [**2**]Tf_2N (393–273 K), and (c) [**3**]Tf_2N (423–473 K). The spectrum at 423 K in (c) is that of the solid state.

Magnetic susceptibilities

The temperature dependence of the magnetic susceptibilities of [**1**]Tf_2N and [**2**]Tf_2N was measured to investigate the change in magnetic properties associated with the thermochromism in the liquid state. Further, the ratios of the open and closed forms, as well as the equilibrium constants, were determined from the data.

The spin state of the thermochromic nickel(II) complexes depends on their coordination structure. The square-planar four-coordinate complex exhibits a low spin state (diamagnetic, S = 0), whereas the five- or six-coordinate complex exhibits a high spin state (paramagnetic, S = 1).[13] Therefore, the ratio of open and closed forms can be determined from the magnetic susceptibility value at each temperature, from which the equilibrium constant (K) for the scheme in Figure 1 can be

calculated. The changes of enthalpy (ΔH), Gibbs free energy (ΔG), and entropy (ΔS) can then be derived from the equilibrium constant using the van't Hoff equation and the relationship $\Delta G = -RT \ln K$.

The temperature dependence of the magnetic susceptibilities of [**1**]Tf_2N and [**2**]Tf_2N is shown in Figure 7. In the case of [**1**]Tf_2N, the $\chi_M T$ value increases gradually with decreasing temperature, which correspond to an increase in the ratio of the paramagnetic closed form. The $\chi_M T$ value becomes nearly constant below the glass transition temperature, consistent with freezing the equilibrium. The magnetic susceptibility value corresponds to the ratio of the closed form, considering the reported value of $\chi_M T$ = 1.2 (μ_{eff} ~ 3.1 B.M.) for the related paramagnetic species.[16] The ratios of the open to closed species were thus found to be 0.76:0.24 at 350 K, 0.69:0.31 at 300 K, and 0.50:0.50 at T_g. The thermodynamic parameters for the equilibrium derived from the data are ΔH = −7.1 kJ mol^{-1} and ΔS = −30.5 J K^{-1} mol^{-1}. The value of ΔS seems to be reasonable for the open–closed transformation, considering that the conformational changes of the alkyl chains provide an entropy change of about 9 J K^{-1} mol^{-1} (= R ln 3) per methylene unit and that the chain contains three methylene groups and an ethoxy group. There is also a contribution of the spin entropy change (R ln 3).

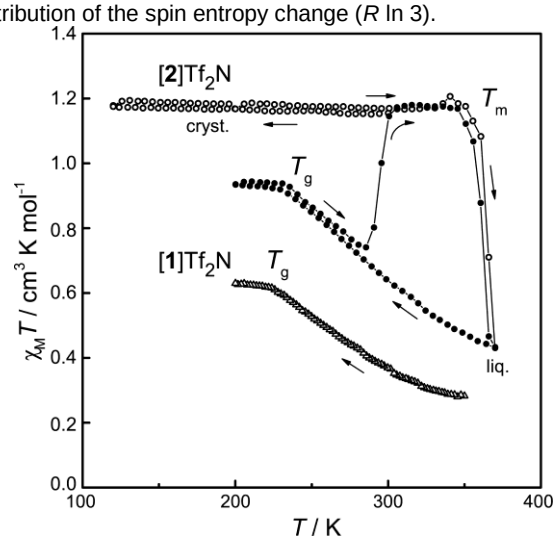

Figure 7. Temperature dependence of the magnetic susceptibilities of [**1**]Tf_2N (△) and [**2**]Tf_2N (○: first cycle; ●: second cycle). Arrows are guides for the measurement sequence.

In the case of [**2**]Tf_2N, the $\chi_M T$ value in the solid state (1.17 cm^3 K mol^{-1}) is temperature independent (Figure 7) and corresponds to the value of the closed form. The susceptibility exhibits a sharp plunge at the melting point owing to a surge in the amount of the open form in the liquid phase. Upon cooling the liquid, the susceptibility increases owing to an increase in the ratio of the closed form in the equilibrium. The susceptibility becomes nearly constant below the glass transition temperature. Upon heating again, the magnetic susceptibility traces back until a sharp increase occurs at 285 K, owing to crystallization, and reaches the value of the solid state.

The ratios of the open and closed species in [**2**]Tf_2N in the liquid state, calculated from the magnetic susceptibility values, were 0.63:0.37 at 370 K, 0.50:0.50 at 310 K, and 0.22:0.78 at T_g. The thermodynamic parameters derived from the equilibrium constants are ΔH = −10.5 kJ mol^{-1} and ΔS = −33.4 J K^{-1} mol^{-1}. The larger negative value of ΔH for [**2**]Tf_2N compared with that for [**1**]Tf_2N is consistent with the smaller steric hindrance of the ether group in [**2**]Tf_2N, which stabilizes the closed form.

Thermochromism in solution

The solvatochromism and thermochromism of [**2**]Tf_2N were examined in solution to investigate the effects of anion and solvents. [**2**]Tf_2N exhibited solvatochromism, showing red in CH_2Cl_2 (DN = 0[17]), light blue in acetone (DN = 17.0[17]), and green in DMSO (DN = 29.8[17]). This phenomenon is typical of the solvatochromic mixed-ligand nickel complexes, whose color change is ascribed to solvent coordination.[2] In the Vis-NIR spectra in each solvent (Figure S1b, Supporting Information), with increasing solvent DN, the peak of the four-coordinate species (λ_{max} = 490 nm) becomes weaker and even disappears in DMSO, whereas the peaks of the five- or six-coordinate species (λ_{max} = 610 and 1000 nm) become stronger.

[**2**]Tf_2N also exhibited thermochromism in solution. The temperature dependence of the Vis-NIR spectra in dichloromethane is shown in Figure 8a. With decreasing temperature, the peaks of the four-coordinate species decrease and those of the five- or six-coordinate species increase. The spectral feature resembles that of neat [**2**]Tf_2N, though the peaks of the latter species are much stronger in solution. The difference is probably ascribed to the coordination ability of the Tf_2N anion, as supported by the spectra of a dichloromethane solution of [**2**]BPh_4, having a non-coordinating anion (Figure 8b). The solution of [**2**]BPh_4 also exhibited thermochromism, but the ratio of the four-coordinate species is much larger than that of [**2**]Tf_2N. Enhanced ion pair formation with Tf_2N in such non-polar solvents may be responsible for anion coordination. Anion coordination might also occur in the neat state, but the effect may be smaller, as seen from the spectra. The spectra of [**2**]BPh_4 in dichloromethane showed a broad absorption at 1000 nm, which could be assigned to the absorption of five-coordinated species. This absorption band closely resembles that of the six-coordinate species, and hence it is difficult to distinguish them through Vis-NIR spectra in the present complexes. On the other hand, the spectrum of the five-coordinated complex [Ni(acac)(pmdt)]BPh_4 (pmdt = *N,N,N′,N″,N″*-pentamethyldiethylenetriamine) in CH_2Cl_2 exhibits weak absorption peaks near 950 nm and 764 nm, which are regarded as characteristic absorptions of this five-coordinated species.[18]

Acetone solutions of [**2**]Tf_2N and [**2**]BPh_4 also exhibited thermochromism (Figure S2, Supporting Information), with a much smaller ratio of the four-coordinate species owing to solvent coordination.

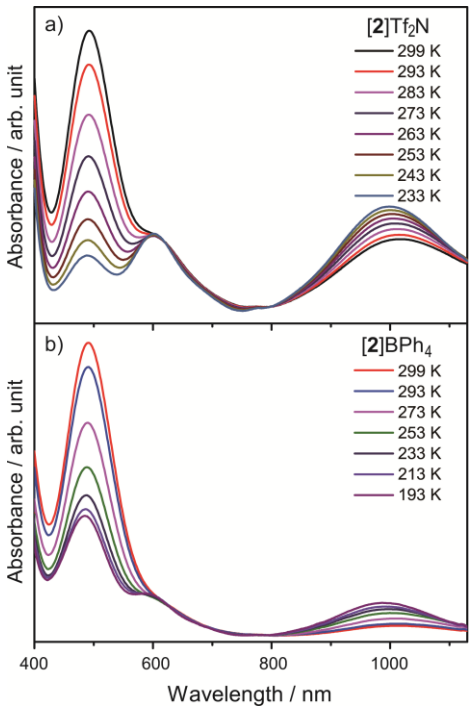

Figure 8. Temperature dependence of the Vis-NIR spectra of (a) [**2**]Tf_2N (299–233 K) and (b) [**2**]BPh_4 (299–193 K) in dichloromethane.

Crystal structures

The crystal structures of water-coordinated complexes [**1**(H_2O)]Tf_2N and [**2**(H_2O)]BPh_4 were determined at 100 K. They were obtained by recrystallization from solvents and found to be solvate crystals containing water and ethanol molecules, respectively. Structural analysis revealed octahedral coordination of the cations, in accordance with their light-blue color.

The molecular structure of the cation in [**1**(H_2O)]Tf_2N is shown in Figure 9a, in which coordination of the ether side chain and a water molecule is seen. The coordination planes formed by the diamine ligand and the acac ligand are perpendicular to each other. The coordination geometry, with two chelate ligands in perpendicular configuration, resembles that in a water-coordinated complex [Ni(tmen)(acac)(H_2O)$_2$]ClO_4 (tmen = *N*,*N*,*N*′,*N*′-tetramethylethylenediamine).[19] The molecular arrangements of the cation and anion are shown in Figure 10. The anion adopts transoid conformation and exhibits two-fold disorder of the central part, as is frequently observed in salts with Tf_2N.[20] The terminal trifluoromethyl moieties in the anion also exhibit rotational disorder over two sites. The solvate water molecule forms hydrogen bonds with the coordinating water (O...O distance: 2.68 Å), an oxygen atom of acac (2.73 Å), and an oxygen of the anion (2.89 Å). The coordinating water also has a hydrogen bond with an oxygen atom of the anion (2.77 Å). The cations and anions are arranged in one-dimensional chains through these hydrogen bonds.

The molecular structure of the cation in [**2**(H_2O)]BPh_4 is shown in Figure 9b. The coordination geometry is essentially the same as that in [**1**(H_2O)]Tf_2N, whereas the acac moiety is disordered. The solvate ethanol molecule is disordered over two sites, which are hydrogen bonded to the coordinating water molecule, the oxygen atom of the acac ligand, and an adjacent ethanol molecule (Figure S3, Supporting Information; O...O distances: 2.71–2.73 Å).

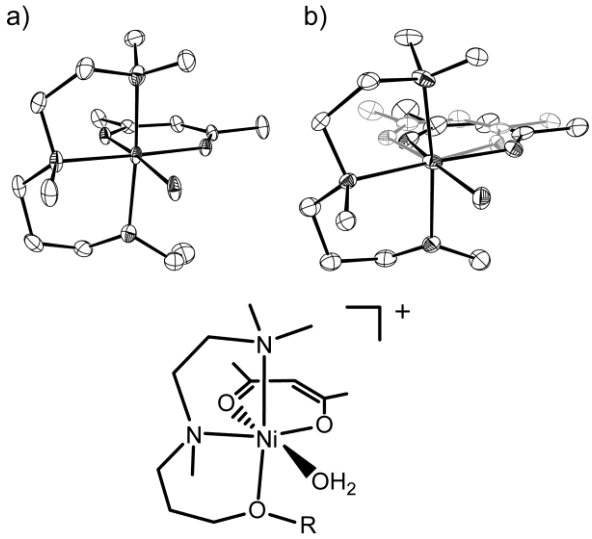

Figure 9. Ortep drawing of the molecular structure of cations in (a) [**1**(H_2O)]Tf_2N·H_2O and (b) [**2**(H_2O)]BPh_4·EtOH. Hydrogen atoms have been omitted for clarity. The disordered moieties are depicted in gray. The structural formula of the cations is shown below (R = Et or Me).

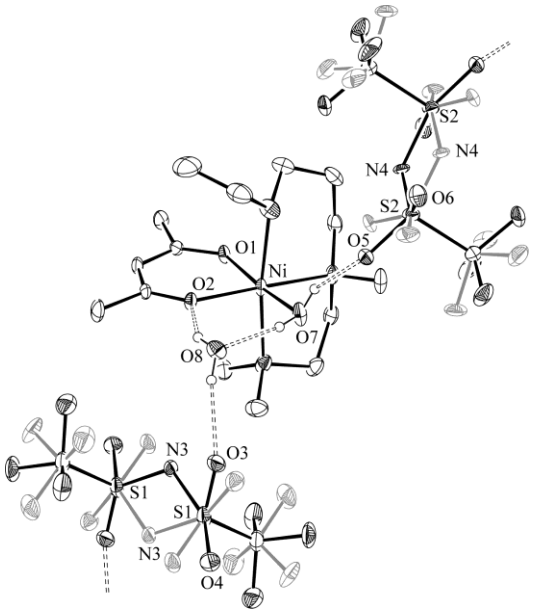

Figure 10. Molecular arrangement in the crystal of [**1**(H_2O)]Tf_2N·H_2O formed through hydrogen bonds. Hydrogen bonds are depicted by dotted lines. Hydrogen atoms, except for those on water, are omitted. The disordered moieties are depicted in gray.

Conclusions

We synthesized ILs that exhibit thermochromic properties and a concomitant change in magnetic properties. The molecular design lies in the use of solvatochromic cationic nickel complexes with ether side chains. The cations can tautomerize between red diamagnetic square-planar four-coordinate species (open form) and blue paramagnetic species with intramolecular side chain coordination (closed form). In the solid state, these salts adopt the closed form, exhibiting bluish colors; however, they form an equilibrium mixture in the liquid state, whose color depends on the ratio of the two species, changing from red at high temperatures to orange, light blue, or bluish green at lower temperatures, depending on the complex. The use of an ether side chain with appropriate coordinating ability is crucial for the mechanism. The thermodynamic parameters for the equilibrium derived from magnetic data are consistent with the molecular structures.

ILs exhibit interesting thermodynamic phenomena related to conformational changes of the constituent molecules.[21] Our original interest in fabricating these ILs was to obtain insight into the effect of large conformational changes on their thermodynamical behavior, and this point is for future investigation. The thermochromism of metal complexes or metal salts is well known, but has been observed in solution or with additives. Thermochromic ILs from metal complexes may be useful for future applications owing to their ionic liquid characteristics such as non-volatility and ionic conductivity, and additional magnetic functions may lead to interesting phenomena.

Experimental Section

General

N′-(3′-Methoxy)propyl-*N*,*N*,*N*′-trimethylethylenediamine (L^2) was synthesized as described in the literature.[6] ^{1}H NMR spectra were recorded on a JEOL JNM-ECL-400 spectrometer. Elemental analyses were carried out on a PerkinElmer 2400II elemental analyzer. DSC measurements were performed using a TA Q100 differential scanning calorimeter at a scan rate of 10 K min^{-1}. The dehydrated sample of [**1**]Tf_2N was sealed in an aluminum pan under an argon atmosphere in a glove box. IR spectra were acquired via attenuated total reflectance using a Thermo Scientific Nicolet iS5 spectrometer. Vis-NIR spectra were recorded on a JASCO V-570 UV/Vis/NIR spectrometer. The spectra of neat samples were recorded under a nitrogen atmosphere. Magnetic susceptibilities were measured using a Quantum Design MPMS-XL7 SQUID magnetometer under a magnetic field of 0.5 T at scan speeds of 2–5 K min^{-1}. Aluminum sample pans were used for the measurements. For SQUID measurements of [**1**]Tf_2N, dehydration of a water solvate sample was carried out at 350 K for 1 h under vacuum inside the sample chamber.

Synthesis of ligands

***N*′-(3′-Ethoxy)propyl-*N*,*N*,*N*′-trimethylethylenediamine (L^1).** *N*,*N*,*N*′-Trimethylethylenediamine (0.612 g, 6.00 mmol) was dissolved in acetonitrile (25 mL) containing anhydrous sodium carbonate (0.742 g, 7.00 mmol) and heated to reflux under a nitrogen atmosphere. A solution of 1-chloro-3-ethoxypropane (0.732 g, 6.00 mmol) in acetonitrile (10 mL) was then added dropwise. Reflux was continued for 1 day, the mixture was cooled and filtered, and the solvent was evaporated. The residue was dissolved in dichloromethane and extracted with water. The organic layer was dried with magnesium sulfate and the solvent was evaporated. Yellow liquid. Yield: 47%. ^{1}H NMR: δ = 1.20 (m, 3 H), 1.75 (m, 2 H), 2.24 (s, 9 H), 2.43 (m, 6 H), 3.45 (m, 4 H). IR: $\tilde{\nu}$ = 2972, 2942, 2856, 2764, 1459, 1376, 1354, 1264, 1187, 1122, 1032, 835 cm^{-1}.

***N*′,*N*′-(3′,3"-Methoxy)dipropyl-*N*,*N*-dimethylethylenediamine (L^3).** This compound was prepared by using the same method as described for L^1, except that *N*,*N*-dimethylethylenediamine (0.528 g, 6.00 mmol) and 1-chloro-3-methoxypropane (1.296 g, 12.00 mmol) were used and reflux was continued for 2 days. Yellow liquid. Yield: 33%. ^{1}H NMR: δ = 1.71 (tt, *J* = 12.9, 6.4 Hz, 3 H), 1.78 (dt, *J* = 9.7, 6.4 Hz, 1 H), 2.23 (m, 7 H), 2.39 (m, 3 H), 2.53 (ddd, *J* = 14.5, 8.4, 6.4 Hz, 4 H), 2.70 (m, 2 H), 3.33 (m, 6 H), 3.39 (dd, *J* = 10.5, 4.1 Hz, 3 H), 3.45 (m, 1 H). IR: $\tilde{\nu}$ = 2936, 2856, 2814, 2765, 1756, 1457, 1384, 1263, 1196, 1115, 1040, 956, 909, 762 cm^{-1}.

Synthesis of metal complexes

[Ni(L^1)(acac)]Tf_2N ([1]Tf_2N). Acetylacetone (0.050 g, 0.50 mmol), sodium carbonate (0.053 g, 0.50 mmol), and L^1 (0.132 g, 0.70 mmol) were added to a solution of $Ni(NO_3)_2{\cdot}6H_2O$ (0.146 g, 0.50 mmol) in methanol (5 mL) with stirring. After stirring for 30 min, lithium bis(trifluoromethanesulfonyl)amide (0.215 g, 0.75 mmol) was added to the solution, which was stirred for a further 30 min. After concentration, diethyl ether (10 mL) was added to the residue and the solution was washed with water (10 × 12 mL). The organic layer was dried over magnesium sulfate and the solvent was evaporated. The crude liquid was dried under vacuum at room temperature for more than 3 h to remove any trace of solvents. Recrystallization of the salt from a diethyl ether/hexane solution containing a small amount of water produced light-blue hydrate crystals [**1**(H_2O)]$Tf_2N{\cdot}nH_2O$ in a heating process to −10 °C after once cooling the solution to −40 °C. Pure dehydrated product was obtained as a red liquid by drying the hydrate compound under vacuum at 75 °C for 3 h. Yield: ~20%. Elemental analysis calcd (%) for $C_{17}H_{31}N_3O_7NiS_2F_6$ (626.26 g mol^{-1}): C, 32.60; H, 4.99; N, 6.71; found: C, 32.69; H, 5.27; N, 6.75.

[Ni(L^2)(acac)]Tf_2N ([2]Tf_2N). This compound was prepared by using the same method as described for [**1**]Tf_2N, except that L^2 (0.087 g, 0.50 mmol) was used. The crude red liquid was dried under vacuum at 75 °C, cooled to room temperature under air, and then gradual solidification occurred in 30 min. The pure product was obtained after recrystallization from diethyl ether/hexane. Light-blue solid. Yield: ~60%. Elemental analysis calcd (%) for $C_{16}H_{29}N_3O_7NiS_2F_6$ (612.24 g mol^{-1}): C, 31.39; H, 4.77; N, 6.86; found: C, 31.12; H, 4.71; N, 6.85.

[Ni(L^3)(acac)]Tf_2N ([3]Tf_2N). This salt was prepared by using the same method as that for [**1**]Tf_2N, except that L^3 (0.116 g, 0.50 mmol) was used. The pure product was obtained by recrystallization after cooling of a diethyl ether/hexane solution gradually to −40 °C. Bluish-green solid. Yield: ~60%. Elemental analysis calcd (%) for $C_{19}H_{35}N_3O_8NiS_2F_6$ (670.32 g mol^{-1}): C, 34.04; H, 5.26; N, 6.27; found: C, 34.14; H, 5.06; N, 6.28.

[Ni(L^2)(acac)]BPh_4 ([2]BPh_4). This salt was synthesized by using the same method as that for [**2**]Tf_2N, except that sodium tetraphenylborate (0.246 g, 0.70 mmol) was used and the crude solution was washed with water nine times. The red liquid turned to a purple solid when cooled gradually under vacuum. The pure product was obtained after

recrystallization from dichloromethane/hexane. Transparent by-products were removed under a microscope. Light-blue solid. Yield: ~30%. Elemental analysis calcd (%) for $C_{38}H_{52}O_{4.5}N_2BNi$ (= [**2**(H_2O)]BPh_4·0.5H_2O, 678.35 g mol^{-1}): C, 67.28; H, 7.73; N, 4.13; found: C, 67.06; H, 7.82; N, 4.28. The sample was dehydrated by heating at 80 °C for 3 h under vacuum to give a red liquid of [**2**]BPh_4, which turned to a violet solid at room temperature. The dehydrated solid was used for solvatochromic measurements in solution. The sample was handled under a nitrogen atmosphere to avoid water absorption.

X-ray structure analysis

Single crystals of [**1**(H_2O)]Tf_2N·H_2O suitable for X-ray crystallography were obtained by recrystallization from a diethyl ether/hexane solution containing a small amount of water at −10 °C. Single crystals of [**2**(H_2O)]BPh_4·EtOH were grown by recrystallization from ethanol. X-ray diffraction data were collected on a Bruker APEX II Ultra CCD diffractometer using MoKα radiation (λ = 0.71073 Å). The structures were solved by the direct method (SHELXS 97).[22] Ortep-3 for Windows was used to produce molecular graphics.[23] Crystallographic parameters are listed in Table 2. CCDC 1503830 ([**1**(H_2O)]Tf_2N·H_2O) and 1503831 ([**2**(H_2O)]BPh_4·EtOH) contain the supplementary crystallographic data for this paper. These data can be obtained free of charge from The Cambridge Crystallographic Data Centre.

Table 2. Crystallographic parameters.

	[**1**(H_2O)]Tf_2N·H_2O	[**2**(H_2O)]BPh_4·EtOH
Empirical formula	$C_{17}H_{35}F_6N_3NiO_9S_2$	$C_{40}H_{57}N_2O_5BNi$
Formula weight	662.31	715.41
Crystal system	Monoclinic	Monoclinic
Space group	$P2_1/n$	$C2/c$
a / Å	8.4307(11)	38.408(13)
b / Å	20.546(3)	10.309(4)
c / Å	16.869(2)	22.951(8)
β / deg	96.951(2)	121.063(4)
V / Å^3	2900.5(7)	7785(5)
Z value	4	8
ρ_{calcd} / g cm^{-3}	1.517	1.221
F (000)	1376	3072
Reflections collected	16544	20847
Independent reflections	6620	8202
Parameters	464	554
Temperature / K	100	100
R_1[a], R_w[b] ($I > 2\sigma$)	0.0756, 0.1673	0.0475, 0.1211
R_1[a], R_w[b] (all data)	0.0775, 0.1682	0.0571, 0.1275
Goodness of fit	1.196	1.031

[a]$R_1 = \Sigma||F_o| - |F_c|| / \Sigma|F_o|$. [b]$R_w = [\Sigma w (F_o^2 - F_c^2)^2/\Sigma w (F_o^2)^2]^{1/2}$

Acknowledgements

This work was financially supported by JSPS KAKENHI (grant number 16H04132). We thank Prof. H. Fujimori (Nihon University) for thermal and spectroscopic investigation on [**1**]Tf_2N and T. Tominaga (Kobe University) for his help with X-ray structure analysis of [**1**(H_2O)]Tf_2N·H_2O.

Keywords: Ionic liquids • Themochromism • Thermal properties • Magnetic properties • Chelates

[1] a) A. Samat, V. Lokshin in *Organic Photochromic and Thermochromic Compounds*, *Vol. 2* (Eds.: J. C. Crano, R. J. Guglielmetti), Springer, New York, **1999**, pp. 415–466; b) *Thermochromic and Thermotropic Materials* (Eds.: A. Seeboth, D. Lötzsch), Pan Stanford, Singapore, **2013**; c) *Thermochromic Phenomena in Polymers* (Eds.: A. Seeboth, D. Litzsch), **2008**, Smithers Rapra Technology; d) M. Ferrara in *Materials that Change Color* (Eds.: M. Ferrara, M. Bengisu), **2014**, Springer International Publishing, pp. 9–60.

[2] W. Linert, A. Kleiner in *Inorganic Chromotropism* (Ed.: Y. Fukuda), Kodansha Ltd., Tokyo, **2007**, pp 40–77.

[3] A. Stark, K. R. Seddon, in *Kirk-Othmer Encyclopedia of Chemical Technology*, Wiley-Interscience, New York, 5th edn, **2007**, vol. 26, pp. 836–919.

[4] a) A. Kawai, D. Kawamori, T. Monji, T. Asaka, N. Akai, K. Shibuya, *Chem. Lett*. **2010**, *39*, 230–231; b) H. Tamura, Y. Shinohara, T. Arai, *Chem. Lett*. **2010**, *39*, 240–241.

[5] A. Branco, L. C. Branco, F. Pina, *Chem*. *Commun*. 2011, 47, 2300–2302.

[6] X. Lan, H. Hosokawa, Y. Funasako, T. Mochida, *Eur. J. Inorg. Chem.* **2016**, *17*, 2804–2809.

[7] Y. Funasako, T. Mochida, K. Takahashi, T. Sakurai, H. Ohta, *Chem. Eur. J.* **2012**, *18*, 11929–11936.

[8] a) N. Aoyagi, K. Shimojo, N. R. Brooks, R. Nagaishi, H. Naganawa, K. Van Hecke, L. V. Meervelt, K. Binnemans, T. Kimura, *Chem. Commun.*, **2011**, *47*, 4490–4492; b) M. Okuhata, Y. Funasako, K. Takahashi, T. Mochida, *Chem. Commun.* **2013**, *49*, 7662–7664.

[9] a) X. Wei, L. Yu, D. Wang, X. Jin, G. Z. Chen, *Green Chem.* **2008**, *10*, 296–305; b) S. J. Osborne, S. Wellens, C. Ward, S. Felton, R. M. Bowman, K. Binnemans, M. Swadźba-Kwaśny, H. Q. N. Gunaratne, P. Nockemann, *Dalton Trans.* **2015**, *44*, 11286–11289; c) Y. Kohno, M. G. Cowan, M. Masuda, I. Bhowmick, M. P. Shores, D. L. Gin, R. D. Noble, *Chem. Commun*. **2014**, *50*, 6633–6636.

[10] a) Y. Yoshida, G. Saito, in *Ionic Liquids: Theory, Properties, New Approaches*, ed. A. Kokorin, InTech, **2011**, 723–738; b) S. Zhang, Q. Zhang, Y. Zhang, Z. Chen, M. Watanabe, Y. Deng, *Prog. Mater. Sci.* **2016**, *77*, 80–124; c) K. D. Clark, O. Nacham, J. A. Purslow, S. A. Pierson, J. L. Anderson, *Anal. Chim. Acta* **2016**, *934*, 9–21.

[11] W. Linert, Y. Fukuda, *Trends Inorg. Chem.* **1999**, *6*, 19–49

[12] Y. Fukuda, K. Sone, *J. Inorg. Nucl. Chem.* **1972**, *34*, 2315–2328

[13] W. Linert, Y. Fukuda, A. Camard, *Coord. Chem. Rev.* **2001**, *218*, 113–152.

[14] a) J. Timmermans, *J. Phys. Chem. Solids* **1961**, *18*, 1–8; b) J. N. Sherwood, *The Plastically Crystalline State: Orientationally Disordered Crystals*, Wiley, Chichester, UK, **1979**.

[15] W. Linert, A. Camard, M. Armand, C. Michot, *Coord. Chem. Rev.*, **2002**, *226*, 137–141.

[16] Y. Fukuda, K. Sone, *J. Inorg. Nucl. Chem.* **1975**, *37*, 455–460.

[17] V. Gutmann, *Coord. Chem. Rev.* **1976**, *18*, 225–255.

[18] A. Taha, W. Linert, Y. Fukuda, *J. Coord. Chem.*, **1993**, *30*, 53–62.

[19] M. Oguni, T. M. Yoshida, K. Wada, Y. Fukuda, N. Ogino, T. Ito, H. Miyamae, K. Sato, *J. Phys. Chem. Solids* **2001**, *62*, 613–618.

[20] W. A. Henderson, M. Herstedt, V. G. Young, Jr., S. Passerini, H. C. De Long, P. C. Trulove, *Inorg. Chem*., **2006**, *45*, 1412–1414.
[21] T. Endo, T. Kato, K. Tozaki, K. Nishikawa, *J. Phys. Chem. B*, **2010**, *114*, 407–411.
[22] G. M. Scheldrick, *Acta Crystallogr., Sect. D: Biol. Crystallogr.* **2008**, *64*, 112–122.
[23] ORTEP-3 for Windows: L. J. Farrugia, *J. Appl. Crystallogr.* **1997**, *30*, 565.

FULL PAPER

Thermochromic magnetic ionic liquids: Thermochromic liquids have been designed based on cationic metal–chelate complexes. These liquids exhibit color changes between red at high temperatures and orange, blue, or blueish-green at lower temperatures depending on the cation. This phenomenon is based on temperature-dependent coordination equilibrium. The thermochromism accompanies changes in the magnetic properties.

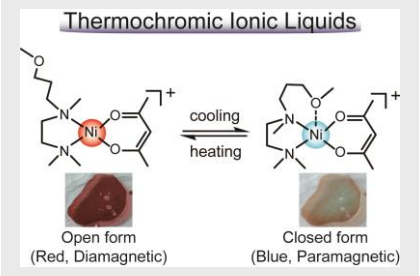

Xue Lan, Tomoyuki Mochida, Yusuke Funasako, Kazuyuki Takahashi, Takahiro Sakurai, and Hitoshi Ohta

Page No. – Page No.

Thermochromic Magnetic Ionic Liquids from Cationic Nickel(II) Complexes Exhibiting Intramolecular Coordination Equilibrium

Electronic Supporting Information

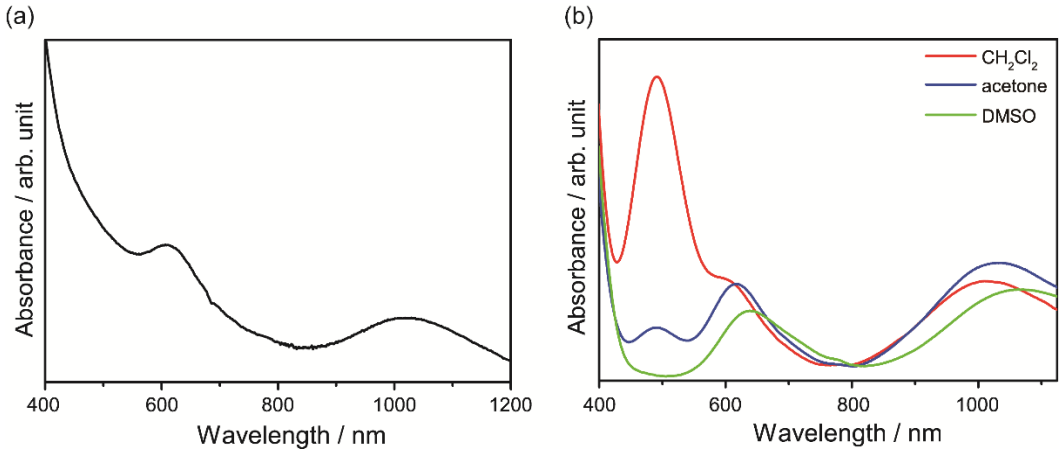

Figure S1. Vis-NIR absorption spectra of [**2**]Tf_2N (a) in the solid state (KBr plates) and (b) in dichloromethane, acetone, and DMSO solutions at room temperature.

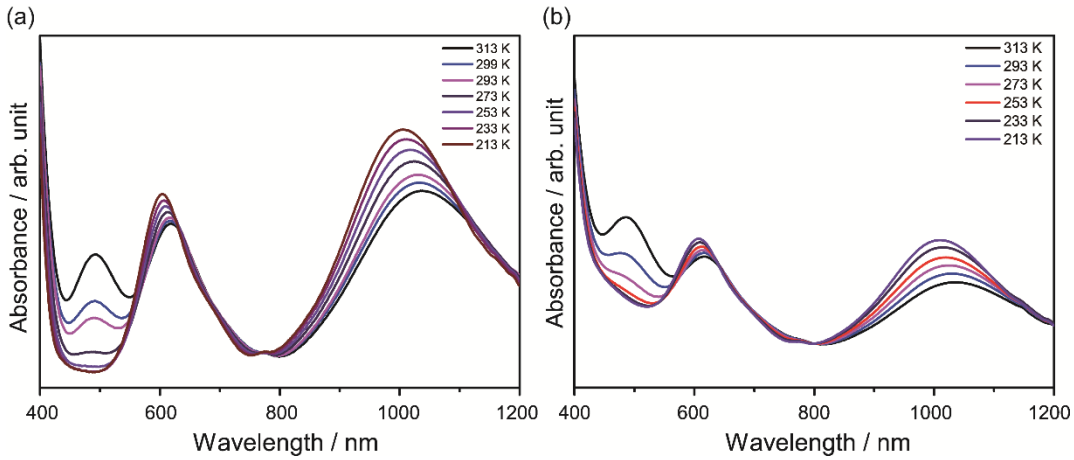

Figure S2. Temperature dependence of the Vis-NIR spectra of (a) [**2**]Tf_2N and (b) [**2**]BPh_4 in acetone.

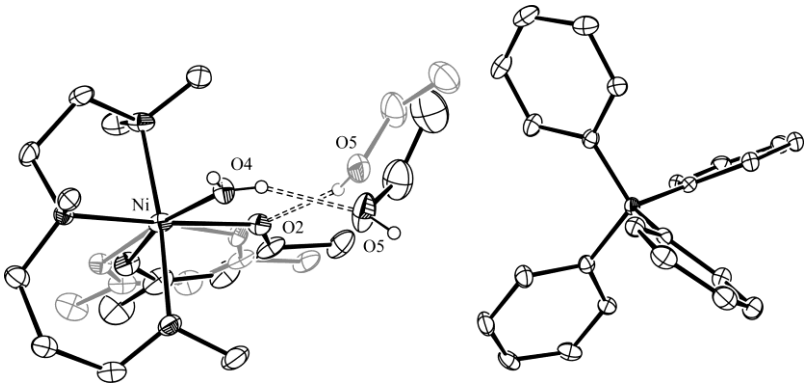

Figure S3. Molecular arrangements in the crystal of [**2**(H_2O)]BPh_4·EtOH. Hydrogen bonds are depicted by dotted lines. Hydrogen atoms, except for those on water, are omitted. The disordered moieties are depicted in gray.